Explanation of Inconsistencies in the Determination of Human Serum Albumin Thermal Stability

Michal Nemergut[1], Dagmar Sedláková[2], Gabriela Fabriciová[3], Dominik Belej[3], Daniel Jancura[3], Erik Sedlák[1,4*]

[1] Center for Interdisciplinary Biosciences, P. J. Šafárik University in Košice, Jesenná 5, 04154 Košice, Slovakia

[2] Department of Biophysics, Institute of Experimental Physics, Slovak Academy of Sciences, Watsonova 47, 040 01 Košice, Slovakia

[3] Department of Biophysics, Faculty of Science, P. J. Šafárik University in Košice, Jesenná 5, 04154 Košice, Slovakia

[4] Department of Biochemistry, Faculty of Science, P. J. Šafárik University in Košice, Moyzesova 11, 04154 Košice, Slovakia

* Corresponding author: erik.sedlak@upjs.sk

Abstract

Thermal denaturation of human serum albumin has been the subject of many studies in recent decades, but the results of these studies are often conflicting and inconclusive. To clarify this, we combined different spectroscopic and calorimetric techniques and performed an in-depth analysis of the structural changes that occur during the thermal unfolding of different conformational forms of human serum albumin. Our results showed that the inconsistency of results in the literature is related to the different quality of samples in different batches, methodological approaches and experimental conditions used in the studies. We confirmed that the presence of fatty acids (FAs) causes a more complex process of the thermal denaturation of human serum albumin. While the unfolding pathway of human serum albumin without FAs can be described by a two-step model, consisting of subsequent reversible and irreversible transitions, the thermal denaturation of human serum albumin with FAs appears to be a three-step process, consisting of a reversible step followed by two consecutive irreversible transitions.

Keywords: serum albumin; protein thermal stability; Lumry-Eyring model; thermodynamic and kinetic stability; phase diagram method

1. Introduction

As the most abundant protein in blood plasma, human serum albumin (HSA) is involved in several vital physiological processes, including maintaining oncotic pressure and transport of various endogenous and exogenous compounds through the circulatory system [1–3]. HSA is of great interest to the pharmaceutical industry thanks to its ability to bind a wide range of small molecules and a long plasma half-life [4–8]. These properties in combination with the presence of multiple ligand-binding pockets make HSA an attractive drug delivery vehicle [9–11]. In addition, HSA represents a well-accepted and established fusion protein partner for improving the pharmacokinetics of short-lived therapeutic proteins [12–14].

HSA is formed by a single polypeptide chain of 585 amino acids arranged in a characteristic heart shape with three homologous α-helical domains (I, II and III) [15,16]. Each domain is composed of two antiparallel six-helix and four-helix subdomains A and B, respectively [17]. The single tryptophan residue (W214) of HSA is located in subdomain IIA [18,19]. According to X-ray structures, seven binding sites for different types of fatty acids (FAs) are distributed asymmetrically across all three domains (**Fig. 1**).

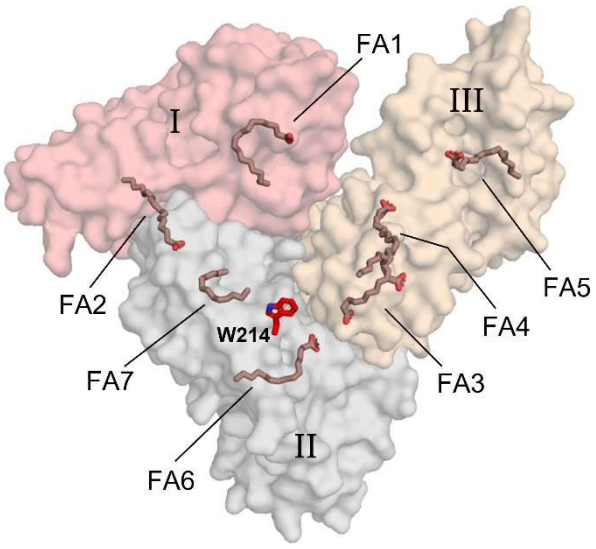

Fig. 1. Schematic representation of HSA showing the three domains and the distribution of fatty acid binding sites (PDB ID: 1GNI). Domains I (**pink**), II (**grey**) and III (**yellow**) are shown in the surface representation and bound fatty acids (**brown**) and W214 (**red**) are shown in the stick representation.

The first FA binding site (FA1) is located in domain I, the two (FA6 and FA7) are in domain II, and the other three (FA3, FA4 and FA5) are found in domain III. The FA2 binding site is located at the interface between domains I and II [20,21]. The highest affinity binding sites are

those located in domain III [22]. The binding of FAs to HSA induces conformational changes involving a rotation of domains I and III relative to domain II [23,24].

As a consequence of a high number of acidic and basic residues, the HSA structure undergoes reversible conformational rearrangement at different pH regions [2]. This can be schematically described by the following scheme:

$$HSA-E \overset{pK_a 2.7}{\longleftrightarrow} HSA-F \overset{pK_a 4.3}{\longleftrightarrow} HSA-N \overset{pK_a 8.0}{\longleftrightarrow} HSA-B \overset{pK_a 10.0}{\longleftrightarrow} HSA-A$$

(Scheme 1)

At neutral and slightly acidic pH (pH 4.3-8.0), HSA exists in its normal heartlike form (HSA-N). Below pH 4.3, HSA assumes a partially expanded cigarlike shape (HSA-F) and upon further reduction in pH to less than 2.7, HSA denatures into its fully extended form (HSA-E) [25]. The most significant structural changes that occur during HSA-N to HSA-F transition take place predominantly in domain III [26–28]. These structural alternations are accompanied by a decrease in α-helical content and an increase in interdomain distances and β-sheet content [26]. In the alkaline pH region (pH 8.0-10.0), HSA is found in its basic form (HSA-B) [29,30]. Above pH 10.0, HSA merges into A form (HSA-A). The transition of HSA-N to HSA-B is characterized by a small decrease in α-helical content and contraction of interdomain distances [26,31,32].

All commercially available albumins must pass through various technological steps during their manufacture. The most frequently used industrial procedure for HSA purification is the Cohn method [33]. This method is based on the fractionation of HSA in ethanol at different pHs followed by the incubation of HSA at ~60 °C for 10 hours in order to inactivate the hepatitis virus [34–36]. It has been shown that this heat treatment of albumin induces its denaturation and aggregation [37–39]. Furthermore, the preparation of bioactive HSA nanoparticles also requires heating the protein [40]. Therefore, it is important to understand the relationship between the HSA structure and thermodynamic parameters describing its thermal stability.

Whereas chemical-induced denaturation of HSA is fully reversible, the thermal unfolding of HSA is only a partially reversible process [41,42]. Wetzel et al. showed that temperature-induced denaturation of HSA is completely reversible up to 65 °C. Upon further heating, this process becomes irreversible with the formation of aggregates [43]. According to Picó, the thermal unfolding of HSA occurs sequentially and can be described by the two-step Lumry-Eyring model [44,45]:

$$Native \overset{K}{\leftrightarrow} Intermediate \overset{k_2}{\rightarrow} Unfolded$$

(Scheme 2)

Later Flora et al. proposed an extended three-step model of temperature-induced denaturation of HSA where the reversible transition from native to expanded form occurs up to 50 °C and represents the separation of domains I and II [46]:

$$Native \overset{K}{\leftrightarrow} Expanded \overset{k_2}{\rightarrow} Intermediate \overset{k_3}{\rightarrow} Unfolded$$

(Scheme 3)

Further heating up to 70 °C leads to irreversible denaturation of domain II. The last step demonstrates the unfolding of domain I at a temperature above 70°C while the denaturation of domain I begins after the completed denaturation of domain II [46]. Although the proposed model describes the multi-step unfolding pathway of HSA thermal denaturation, it does not include the unfolding of domain III. On the other hand, Ahmad et al. found that the temperature-induced unfolding of HSA-N and HSA-B forms is a cooperative process while the unfolding of the HSA-F form is a non-cooperative process [47]. In addition, several other studies showed that thermal denaturation of HSA follows different unfolding pathways, including the intermediate state within domain III [48–51]. Despite extensive research on the thermal denaturation of HSA, the results from these studies remain conflicting and inconclusive.

In this work, we provide a comprehensive mathematical model that allows clarification of inconsistencies concerning the temperature denaturation of both HSA with and without fatty acids. Combining different spectroscopic and calorimetric methodical approaches, we perform an in-depth analysis of structural changes that occur during the thermal unfolding of distinct HSA conformational forms.

2. Materials and methods

2.1. *Materials*

Both HSA without (A-3782) and HSA with (A-8763) fatty acids were purchased from Sigma-Aldrich, Germany. Different forms of HSA were prepared in 10 mM buffers: glycine (pH 3.3), sodium acetate (pH 4.0), cacodylic acid (pH 6.5), phosphate buffer (pH 7.0 and pH 7.4) and N-cyclohexyl-2-aminoethanesulfonic acid (pH 9.0 and pH 10.0).

2.2. *Sample preparation*

The samples were incubated twelve hours before the experiments. The pH values of all samples were determined before as well as after the measurements and no changes were detected.

Protein concentration was measured spectroscopically with the following parameters: Mw = 66.5 kDa, ε_{280} = 36500 M^{-1} cm^{-1}.

2.3. *Circular dichroism (CD) measurements*

Jasco J-810 spectropolarimeter (Tokyo, Japan) equipped with a Peltier-type thermostated single-cell holder (PTC-423S) was used for circular dichroism measurements. Ellipticities were measured at 222 nm in 0.1 cm pathlength quartz cuvette. The temperature was continuously varied from 20 to 100 °C with a heating rate of 1.5 °C/min. The protein concentrations were 0.5 mg/ml (8.0 μM) in all experiments.

2.4. *Fluorescence measurements*

Fluorescence experiments were performed on a Varian Cary Eclipse fluorescence spectrophotometer (Varian Australia Pty Ltd) equipped with a Peltier multicell holder. The temperature was changed from 10 to 100 °C with a heating rate of 1.5 °C/min. The excitation wavelength was 295 nm and emission at 350 nm was collected. The protein concentrations were 0.5 mg/ml (8.0 μM) in all experiments.

2.5. *Differential scanning calorimetry (DSC) measurements*

DSC experiments were carried out on a VP-Capillary DSC system (Microcal Inc., acquired by Malvern Instruments Ltd.) at a scan rate of 1.5 °C/min. An extra pressure of 65 psi was maintained during all DSC runs to prevent possible degassing of the solutions during heating. Thermograms were corrected by subtraction of the so-called chemical baseline, i.e., the sigmoidal curve connecting the signal of excess heat capacity of the native and denatured states, and normalized to the molar concentration of the protein. All experiments (except concentration dependence experiments) were performed at a protein concentration of 1.5 mg/ml (22.6 μM).

2.6. *Analysis of CD and fluorescence measurements*

Thermodynamic parameters were determined by fitting experimental data according to the equation describing the two-state process of denaturation:

$$Y_{obs} = \frac{Y_N + S_N.T + (Y_D + S_D.T).e^{\frac{-\Delta H_{vH}(T_M - T)}{R.T_M.T}}}{1 + e^{\frac{-\Delta H_{vH}(T_M - T)}{R.T_M.T}}},$$

(Equation 1)

where Y_N and Y_D represent intercepts of the pre-transition and post-transition baselines with the y-axis, respectively. Slopes of the pre-transition and post-transition baselines are symbolized by S_N and S_D, respectively. The parameter ΔH_{vH} represents an apparent van't Hoff enthalpy at

the transition temperature T_M, R is a gas constant (8.314 J K^{-1} mol^{-1}) and T is temperature. All CD and fluorescence curves were finally normalized with the purpose to compare them with thermograms obtained from the DSC study.

2.7. *Analysis of DSC measurements*

The thermal denaturation of HSA can be described by a two-step Lumry-Eyring model (Scheme 2) [45]. In Scheme 2, K is an equilibrium constant and k_2 is a rate constant of the corresponding step. The excess heat capacity, which is the parameter measured in the DSC experiments, is then expressed by the following equation:

$$C_p^{ex} = -\Delta H_1 \frac{dX_N}{dT} + \Delta H_2 \left(\frac{k_2 X_I}{v}\right),$$

(Equation 2)

where ΔH_1 and ΔH_2 are molar enthalpy changes of the first and second steps, respectively; X_N and X_I are molar fractions of the native and the intermediate states (Equation 2) of the protein, respectively. The parameter v is the scan rate in K/min.

The thermal denaturation of HSA_{FA} can be described by the three-step model expressed by Scheme 3 for which we derived a mathematical equation to express the excess heat capacity [52]. In Scheme 3, K is an equilibrium constant and k_2 and k_3 are rate constants of corresponding steps. The excess heat capacity for this equation is given by:

$$C_P^{ex}(T) = -\Delta H_1 \left(\frac{dX_N}{dT}\right) + \Delta H_2 \left(\frac{k_2 X_E}{v}\right) + \Delta H_3 \left(\frac{k_3 X_I}{v}\right),$$

(Equation 3)

where ΔH_1, ΔH_2, and ΔH_3 are molar enthalpy changes for the first, second and third steps, respectively; X_N, X_E, and X_I are molar fractions of corresponding states of the protein (as defined in Scheme 3) and v is the scan rate in K/min. The rate constant at any given temperature can be obtained from the Arrhenius equation, in the alternative form [45]:

$$k = exp\left[\frac{E_a}{R}\left(\frac{1}{T^*} - \frac{1}{T}\right)\right]$$

where E_a is the energy of activation, R is the gas constant, and the parameter T^* equals the temperature at which the rate constant equals 1 min^{-1}. However, detailed analysis showed that the three-step model describes the thermal transitions of HSA_{FA} only to a limited extent. In fact, the thermal denaturation of HSA_{FA} is a complex process and depends both on the scan rate and the protein concentration. Therefore, the obtained results were utilized only for comparison purposes of kinetic stabilities of HSA_{FA} at the same protein concentration (22.6 μM) and scan rate (1.5 K/min) in analogy with our previous work [53].

3. Results

3.1. *Albumins from different batches exhibit distinct thermal stabilities*

We analyzed thermal denaturation of four different batches of both human serum albumin with (HSA_{FA}) and without fatty acids (HSA) by DSC (**Fig. 2**).

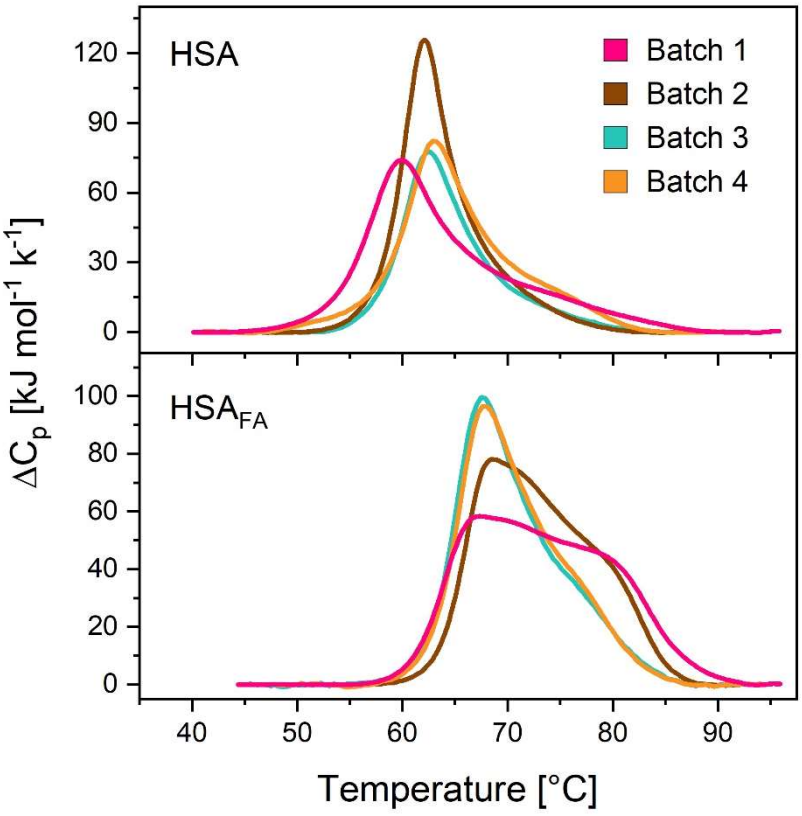

Fig. 2. Comparison of thermal denaturation of HSA (upper panel) and HSA_{FA} (lower panel) from different batches represented by a different color. All measurements were performed at a protein concentration of 1.5 mg/ml and a scan rate of 1.5 °C/min in phosphate buffer with pH 7.4.

A comparison of DSC scans of albumins from different batches obtained under the same conditions clearly demonstrates significant variability in their thermal unfolding. In the case of HSA, the difference in apparent transition temperature (the temperature at heat capacity maximum) between the least stable (pink curve) and the most stable (orange curve) HSA is approximately 3°C. The presence of a small shoulder around 75°C (more pronounced in pink and orange curves) indicates that HSA does not undergo one-step thermal unfolding but the transition from native to the denatured state must proceed through at least a two-step pathway. DSC scans of HSA_{FA} indicate more complex thermal denaturation of albumin-containing FAs compared to albumin without FAs. This is probably due to the interaction of FAs with HSA,

which differs in the stoichiometry as well as binding affinity in the individual domains (**Fig. 1**) [20]. In addition, the binding of FAs may affect not only a stability of the individual domains, as for example FA2 which binds to the interface between domains I and II and thus likely affects stability of both domains [24]. On the other hand, weakening of the FAs-HSA interaction or release of FAs due to a conformational change of the binding site, e.g. by a change in pH and/or temperature, may also lead to changes in the thermograms (**Fig. 2**). As in the case of HSA, the DSC curves of HSA_{FA} from different batches also exhibit a slightly different thermal denaturation profile. At least two of four DSC scans of HSA_{FA} (brown and pink curves) seem to consist of three distinct thermal transitions corresponding to three-step thermal denaturation.

3.2. *Thermal denaturation of albumin is a kinetically controlled multi-step process*

To further investigate the mechanism of thermal denaturation of albumin, we determined whether individual transitions are dependent on protein concentration and heating rate. To simplify the analysis, further measurements were performed only with batch 2 (brown curves), which represents a kind of compromise among the four batches studied. The concentration dependence study of both HSA and HSA_{FA} was carried out with three different protein concentrations, specifically 1, 2 and 3 mg/ml (**Fig. 3,** the upper panel).

The DSC thermograms of HSA are almost identical at all three protein concentrations clearly indicating that the thermal denaturation of HSA is independent of protein concentration. On the other hand, the thermal unfolding of HSA_{FA} is slightly dependent on protein concentration. The increase in the protein concentration causes the shift of the apparent transition temperatures to higher values of approximately 1 °C. Interestingly, with an increase of protein concentration, the first apparent transition is shifted to a higher temperature while the shoulder position seems to be unaffected. This fact indicates the presence of intermolecular interactions, probably due to the formation of dimers with a stabilizing effect on the interacting domains. This is consistent with the tendency of HSA to form reversible dimers via hydrophobic interactions [54]. The formation of such dimers can be induced by various factors, including a high temperature [55–57]. To reveal kinetically driven transitions, we also performed DSC runs at three different scan rates, specifically 1, 2 and 3°C/min (**Fig. 3,** the lower panel). In the case of HSA, there is a slight increase in thermal stability with a rise of the heating rate. This stabilization is accompanied by a decrease in the molar heat capacity change. The presence of bound FAs in the structure of the albumin molecule causes a more complex

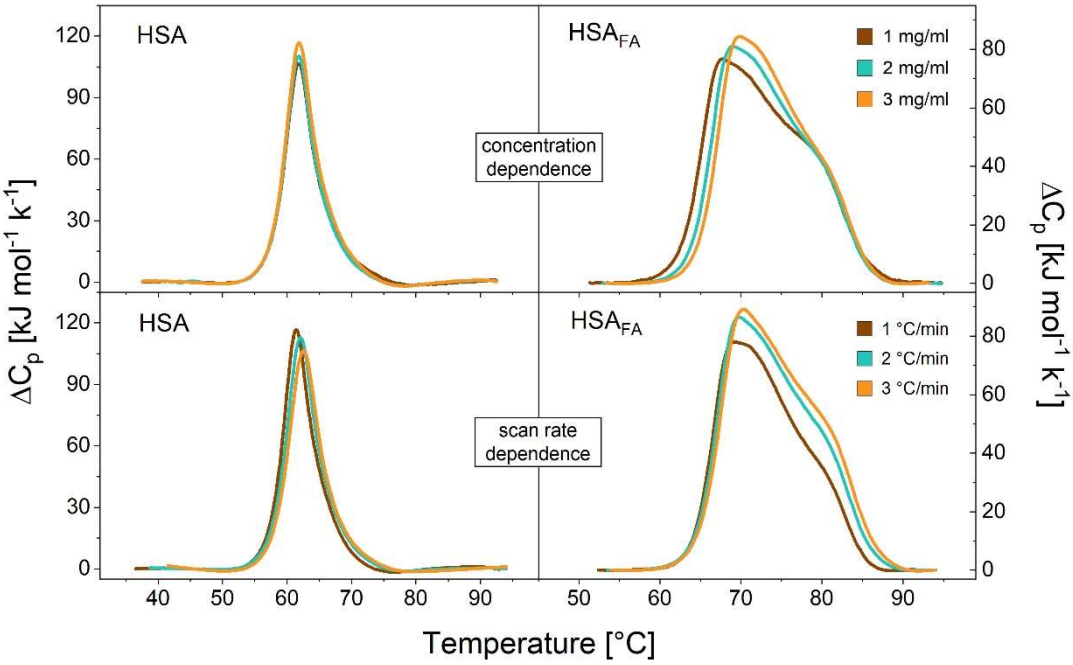

Fig. 3. Concentration (the upper panel) and scan rate (the lower panel) dependence of HSA and HSA_{FA} thermal denaturation. DSC scans corresponding to concentration dependence are shown in **brown** (1.0 mg/ml), **cyan** (2.0 mg/ml) and **orange** (3.0 mg/ml) at a scan rate of 1.5 °C/min. The scan rate dependence is shown in **brown** (1.0 °C/min), **cyan** (2.0 °C/min) and **orange** (3.0 °C/min) at a protein concentration of 1.5 mg/ml. All measurements were carried out in phosphate buffer at pH 7.4.

scan rate dependence of individual transitions. There is a change of the main peak as well as a change of the shoulder. Both these parts are shifted to higher temperatures with increasing of the heating rates. Furthermore, the main peak becomes more uniform during faster thermal denaturation indicating that the main peak consists at least of two intrinsic transitions. These results suggest that the temperature denaturation of HSA and HSA_{FA} probably corresponds to two-step and three-step processes, respectively. (**Fig. S1** and **S2**).

3.3. *The stabilizing effect of FAs is not equal in different albumin conformations*

To find out the stabilizing effect of the bound FAs in the particular conformational forms of HSA, we performed DSC measurements of three different conformational forms HSA-F, HSA-N, and HSA-B, as defined in Scheme 1. Moreover, the denaturation of each form was analyzed at two different pH values within the defined pH range of the form. A comparison of the effect of FAs on the thermal stability of three different conformational forms of both HSA and HSA_{FA} is shown in **Fig. 4**.

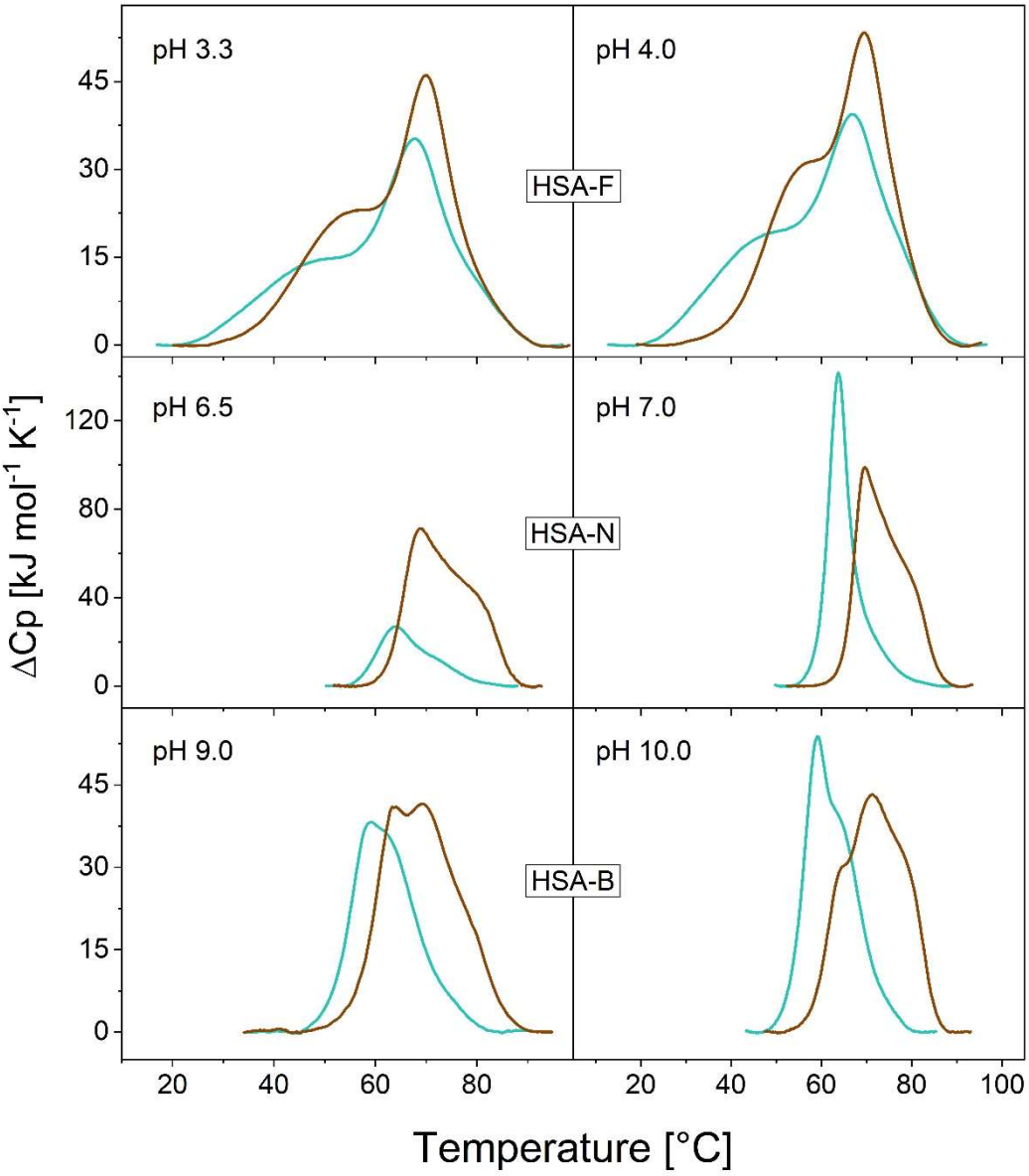

Fig. 4. DSC scans of HSA (**cyan**) and HSA_{FA} (**brown**) in different pH regions. All measurements were performed at a protein concentration of 1.5 mg/ml and a scan rate of 1.5 °C/min in the respective buffers (see Materials and methods). Note the different scales on the y-axes.

The stabilities of the conformational forms of HSA are represented at two pHs in different pH regions, specifically HSA-F form at pH 3.3 and pH 4.0, the HSA-N form at pH 6.5 and pH 7.0 and the HSA-B form at pH 9.0 and pH 10.0. The stabilization effect of FAs was confirmed in all investigated albumin forms. The thermograms of the HSA-F form are broader in comparison with HSA-N and HSA-B forms because of the earlier onset of denaturation. There is no significant difference between DSC scans of HSA-F performed at pH 3.3 and pH 4.0. Both DSC scans consist of the main peak around ~67 °C and the shoulder spanning from

~25 to 55 °C. This shoulder points out the presence of a less stable part of the albumin which begins to denature even at a room temperature. The stabilizing effect of FAs is not as pronounced as in other conformational forms. The most evident stabilization effect of bound FAs is reflected in the stabilization of the region represented by the shoulder at lower temperatures.

Despite only a slight change in pH, there is a noticeable difference in the thermal unfolding between the studied HSA-N forms. While the transition temperatures are the same (~64 °C), the heat capacity change is more than 4 times lower at pH 6.5 than at pH 7.0. Although the isoelectric point of HSA is at pH~5, i.e. relatively distant from pH 6.5, a higher tendency of HSA to aggregate compared to HSA_{FA} at this pH cannot be excluded. This would explain the significantly lower molar heat capacity change observed in the case of HSA-N at pH 6.5 in comparison with the heat capacity change at pH 7.0. Moreover, three shoulders begin to appear at pH 6.5 while the DSC curve seems to be almost symmetrical at pH 7.0. The presence of the shoulders indicates that the HSA-N form at pH 6.5 represents a rather intermediate state between HSA-F and HSA-N forms, suggesting that the pK_a transition between HSA-F and HSA-N is shifted to a more neutral pH for HSA in comparison with HSA_{FA}. On the other hand, DSC scans of the HSA_{FA}-N form share similar features at both pH values. In the presence of FAs, the position of the maximum of the main peak is shifted about 5-6 °C to ~69 °C. The positions of the maximum of the main peaks at pH 6.5 and pH 7.0 are 68.3 °C and 69.6 °C, respectively. Compared to HSA_{FA}-F, there is a loss of the shoulder at a lower temperature (left side) of DSC scans, which suggests the further stabilization of this part of the protein by FAs. In addition, a new shoulder has appeared at the higher temperature (right side) of DSC scans, which indicates an unequal stabilization effect of FAs on the individual domains.

DSC scans of HSA-B form also share similar properties at both pH levels. HSA-B form is characterized by thermograms containing two distinguishable transitions. The shoulders on the right side of the DSC curves are more pronounced with increasing pH, indicating structural changes in HSA that are very likely associated with the conformational transition from HSA-B to HSA-A. At pH 10.0 and in the presence of FAs, the position of the maximum of the main peak is shifted by ~12 °C to higher temperatures (71 °C), which is the most pronounced stabilizing effect of FAs among the studied conformational forms. Moreover, while DSC scans of HSA_{FA}-F and HSA_{FA}-N forms consist of two clearly detectable transitions, DSC scans of HSA_{FA}-B are composed of three apparent transitions.

3.4. *Different conformational forms of albumin exhibit distinct modes of thermal denaturation*

To better understand the structural changes that occur during thermal denaturation of HSA in more detail, two additional spectroscopic methods were used. Changes in the secondary and tertiary structures of the three conformational forms of albumin HSA-F (pH 3.3), HSA-N (pH 7.0) and HSA-B (pH 9.0) were monitored by circular dichroism (CD) and intrinsic tryptophan fluorescence, respectively. The obtained CD and fluorescence curves were normalized and plotted with DSC scans. The apparent transition temperatures determined by fitting experimental data are shown in **Table S1**. A comparison of the thermal unfolding of HSA and HSA_{FA} monitored by DSC, CD and Trp fluorescence is shown in **Fig. 5**.

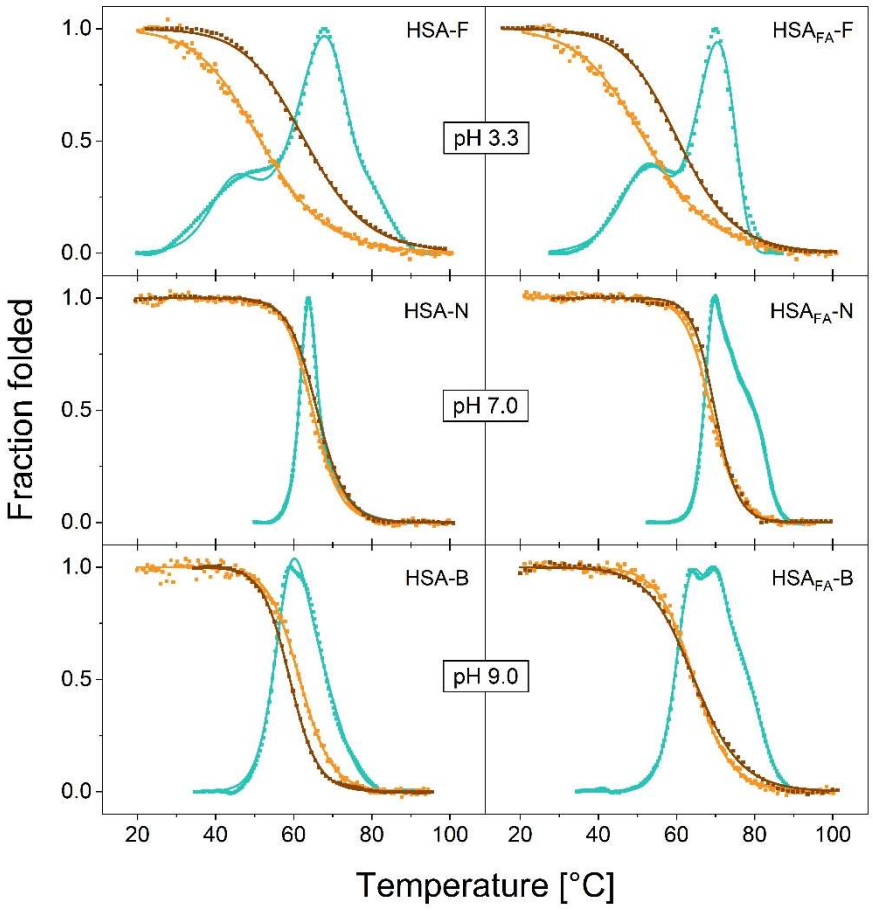

Fig. 5. Comparison of thermal unfolding of three conformational forms of HSA and HSA_{FA} monitored by CD (**orange**) and Trp fluorescence (**brown**) normalized to the corresponding DSC scan (**cyan**). All measurements were performed at a protein concentration of 1.5 mg/ml and a scan rate of 1.5 °C/min in the respective buffers (see Materials and methods). The solid lines represent the fits to corresponding models (two-step model for HSA-N and HSA-B, and three-step model for all other albumin forms). The experimental data are shown as dots.

Analysis of ellipticity and Trp fluorescence curves of both HSA-F and HSA_{FA}-F thermal unfolding revealed the unequal denaturation of the particular domains. Considering that

albumin contains a single tryptophan residue in its structure, measured fluorescence reflects conformational changes of domain II only. A significant difference between ellipticity and Trp fluorescence temperature dependences demonstrates: (i) the existence of (at least) one intermediate in thermal denaturation transition and (ii) that the unfolding of domain II begins at a higher temperature. Thermal denaturation with lower transition temperature observed by CD suggests a destabilization of the secondary structure of both HSA and HSA_{FA} at acidic pH (**Fig. S3**). The temperature ellipticity dependencies of both HSA and HSA_{FA} show nearly identical transition temperatures, ~52 °C. The lower thermal stability of HSA-F and HSA_{FA}-F forms observed by both spectroscopic techniques is consistent with our calorimetric results. In fact, DSC thermograms show that thermal denaturation of both HSA-F and HSA_{FA}-F forms proceeds through (at least) one intermediate and the transition at a lower temperature well correlates with the transition temperatures obtained by CD experiments (**Fig. 5, Tables S1-S3**). Transition temperatures determined by Trp fluorescence for HSA (62.9 °C) and HSA_{FA} (60.5 °C) demonstrate an absence of stabilization effect of FAs on the albumin in the F form. This suggests disruption of the protein tertiary structure at acidic pH to a such degree that FAs do not bind to the albumin (**Fig. S4**).

The complexity of albumin thermal denaturation was also analyzed by using phase diagram methods [58–60]. The basis of this simple but powerful method in revealing hidden intermediates is a pairwise correlation of two different extensive parameters (e.g., spectral intensities) in a plot. For the two-state transition, the plot of the intensities should be linear. Any nonlinearity corresponds to the deviation from an all-or-none transition. The number of linear portions, *n*, indicates n+1 species. This phase diagram method should be applied to data measured under identical conditions. Here, fluorescence emission intensities at 333 and 350 nm (upon excitation at 295 nm) were interrelated and plotted as F_{350} versus F_{333} (**Fig. S5**). In the case of the F forms, the plots are nearly linear, indicating the unfolding of domain II in an all-or-none fashion. This is in agreement with the expected expanded state of albumins at acidic pH. Thermal denaturation of the HSA-N form was found to be seemingly more uniform. Transition temperatures determined by CD (~65 °C) and Trp fluorescence (~66 °C) are in a good agreement with the transition temperature determined by DSC (~64 °C). The excellent overlap of ellipticity and Trp fluorescence temperature dependencies suggests the simultaneous unfolding of individual domains, i.e. two-state transition [61,62]. From the comparison of HSA-N and HSA_{FA}-N forms, the same stabilizing effect of FAs (~5-6 °C) was observed by both spectroscopic techniques and DSC. Transition temperatures of thermal denaturation determined by monitoring ellipticity in the far-UV region and Trp fluorescence correspond to the maximum

of the main peak in DSC scans of HSA_{FA}-N form. The position of the shoulder in thermograms (~80 °C) indicates that there is a part of HSA_{FA}-N, which begins to unfold after the denaturation of domain II. On the other hand, additional analysis of the fluorescence curves showed that the denaturation of HSA-N and HSA_{FA}-N is a multi-step process (**Fig. S5**). The presence of two linears in the phase diagram method in the case of HSA-N and three linears in the case of HSA_{FA}-N strongly indicate two-step and three-step thermal denaturation transitions for corresponding N forms of albumin.

Analogous analysis of HSA-B and HSA_{FA}-B forms leads to conclusions that: (i) both B-forms of albumin are less stable than the N forms and (ii) the thermal transitions of HSA-B and HSA_{FA}-B are two-step and three-step transitions, respectively (**Fig. 5** and **S5**). Moreover, the transition temperature determined from the temperature dependence of Trp fluorescence corresponds to the first transition in the DSC thermogram of both B forms. In the case of HSA-B, the transition temperature determined from Trp fluorescence is lower than the transition temperature determined by CD which clearly indicates that domain II is not the most stable domain in the B forms of albumins.

4. Discussion

Despite extensive research on the thermal denaturation of HSA, the question about the mechanism of this process is still open. A broad range of different techniques has been used to solve this problem, but the results are often contradictory [43,46,63–65,51,49]. In this work, we showed that the thermal denaturation of human serum albumin depends on: (i) the content of FAs, (ii) the scan rate of measurement, and (iii) protein concentration in the case of HSA_{FA}. Human serum albumin represents a quite complex thermodynamic system as it consists of three domains that can be further separated into six subdomains with a varying amount of bound FAs and different binding affinities. The stability of multidomain proteins can significantly depend not only on the domain fold but also on the interdomain interactions [66].

Comparison of transition temperatures in human serum albumin reported in previous studies. A part of the controversy and inconsistency in the results presented in the literature appears to be related to different methodological approaches and experimental conditions used in these studies (**Table 1**).

Table 1: Previous studies investigating thermal denaturation of HSA-N and HSA_{FA}-N.

Author (year)	Protein	Method	Transition temperature (°C)	Protein concentration (mg/ml)	Scan rate (K/min)	pH	Reference
Wetzel (1980)	HSA	CD ESR	71 73	0.5 10	ND	6.0	[43]
Shrake (1984)	HSA_{FA}	DSC	66.8 ± 0.1 78.5 ± 0.1	48	0.25	7.0	[71]
Ross (1988)	HSA_{FA}	DSC	69.1± 0.1 78.0 ± 0.1	5.2	0.25	7.0	[68]
Picó (1997)	HSA	DSC FT	63.2 ± 0.4 62.1 ± 0.3	6 1.3	1 0.7	7.4	[44]
Flora (1998)	HSA	FT	ND	0.07	3	7.2	[46]
Kosa (1998)	HSA	DSC	59.7 ± 0.1	6.7	1	7.4	[50]
Muzammil (1999)	HSA	CD	ND	1.2	ND	6.0	[74]
Farruggia (2001)	HSA	DSC	56.1 ± 0.1 61.6 ± 0.6	10	1	7.4	[63]
Michnik (2006)	HSA	DSC	62.5 ± 0.3 71.9 ± 0.6	5.0	1	6.0	[64]
	HSA_{FA}	DSC	73.4 ± 0.2 82.2 ± 0.2				
Celej (2006)	HSA	DSC	60.1 ± 0.1	7.3	1	7.2	[65]
Rezaei-Tavirani (2006)	HSA_{FA}	DSC	ND	1	1	7.0	[48]
Ahmad (2015)	HSA	CD	ND	0.3	1	7.4	[47]
This work	HSA	DSC CD FT	63.8* 64.8 ± 0.1 66.0 ± 0.1	1.5 0.5 0.5	1.5	7.0	-
	HSA_{FA}	DSC CD FT	69.6* 68.9 ± 0.1 69.9 ± 0.1	1.5 0.5 0.5			

ESR = electron spin resonance; FT = fluorescence techniques; *value corresponding to the main peak in DSC

Another reason for conflicting results can be related to the unequal quality of the samples. Our DSC experiments of four different albumin batches performed under identical conditions clearly showed that the quality of samples varies from batch to batch. Differences in temperature denaturation between samples were found in both HSA and HSA_{FA}. Considering that HSA begins to unfold around 60 °C and that the purification process involves several hours of incubation of HSA at 60 °C, the variability between samples is likely due to the presence of irreversibly denatured fractions of albumin in different batches [36]. The presence of the oligomeric fraction in albumin samples has been shown previously [38,39,67]. In the case of HSA, the differences reflected mainly in the thermal stability and the presence of shoulders in

the DSC curves could be caused by the unequal removal of FAs from the HSA_{FA} structure. Both reasons can be expressed at a different level in albumin batches resulting in observed variability of determined thermodynamic parameters of the protein denaturation.

Contradictory results can be found not only in the values of transition temperatures but also in conclusions about the thermal unfolding pathway of HSA. Ross and Shrake showed that the thermal stability of HSA and the first transition of HSA_{FA} are concentration as well as scan rate dependent while the thermal stability of the second transition of HSA_{FA} depends neither on the concentration nor on the scan rate [68]. On the other hand, Michnik pointed out that the thermal denaturation of HSA_{FA} second transition is concentration-dependent [64]. Further confusion was brought by Picó who claimed that HSA thermal unfolding is scan rate independent [44].

To clarify this, we performed two different types of DSC experiments with both HSA and HSA_{FA}. The first set of DSC experiments was focused on the dependence of the transition temperature on protein concentration. Our results indicate that HSA thermal unfolding does not depend on protein concentration while the thermal unfolding of HSA_{FA} is partially concentration-dependent. The shift of the main peak position to higher temperatures with increasing protein concentration suggests that oligomerization of HSA_{FA} leads to more stable albumin forms [45,53]. These findings are not consistent with the results obtained by Wetzel and Ross who observed a decrease in stability with an increase in the concentration of both HSA and HSA_{FA} [43,68]. However, in these cases, the authors observed the formation of aggregates during the thermal denaturation of HSA which may have affected the denaturation process. The scan rate dependence experiments revealed that the thermal stability of both albumins depends on the heating rate. Our results confirmed also the scan rate dependence of the shoulder in HSA_{FA} which is in conflict with the previous findings mentioned above. On the other hand, the HSA_{FA} scan rate dependence of both the main peak as well as the shoulder reflects the presence of two irreversible transitions, which is in accordance with the proposed three-step model by Flora [46].

Role of fatty acids in thermal stability of human serum albumin. The stabilization effect of bound FAs on the thermal stability of HSA has been shown previously [69–72]. Brandt and Andersson suggested FAs migration from the aggregating molecules to the remaining monomers and thereby stabilizes the latter against heat denaturation [69]. Later Shrake and Ross concluded that biphasic thermal denaturation of HSA_{FA} is due to FAs redistribution during denaturation process [73]. This unequal FAs redistribution leads to the formation of two fractions with lower and higher FAs content which is reflected as less and more stable fractions

of albumin, respectively [71,73]. Even though our DSC experiments confirm the stabilization effect of FAs on HSA, we suggest that the accompanying changes in thermograms are rather related to the denaturation of individual domains than to the presence of albumin fractions with different levels of FAs content. DSC thermograms of HSA_{FA}-B form consist of three distinct transitions that correspond to three subsequent unfolding steps or in other words, four albumin fractions with differently unfolded conformations. Moreover, thermograms of HSA also contain shoulders at all investigated pH values. This disagreement can be explained by the fact that Shrake and Ross performed their measurements only at pH 7.0 where the DSC scan of HSA is seemingly symmetrical and the DSC scan of HSA_{FA} consists of two distinguishable transitions [73]. Next, they showed that palmitate increases the thermal stability of HSA up to the concentration of 6.8 palmitate equivalents per one HSA molecule. Further increase of palmitate concentration did not lead to further stabilization due to saturation of the binding sites. Later Bhattacharya and coworkers confirmed that HSA is able to bind simultaneously seven equivalents of palmitic acids under physiological conditions [20]. All these findings suggest that FAs binding sites are fully occupied under physiological conditions, and therefore a release of FAs during denaturation cannot cause further thermal stabilization. On the other hand, individual domains feature different thermal stability and contain a diverse number of FAs binding sites which can cause changes between HSA and HSA_{FA} thermograms.

Analysis of different pH forms of human serum albumins in the presence and absence of bound fatty acids. To provide a comprehensive characterization of three conformational forms of HSA and HSA_{FA}, we compared the results from CD, Trp fluorescence and DSC experiments. Our results suggest that the least stable conformational form is the HSA-F form. DSC thermograms of this form are composed of the main peak and a less stable shoulder which is consistent with the biphasic thermogram of HSA at pH 4.3 observed by Picó [44]. Spectroscopic techniques revealed changes in the secondary and tertiary structures of the proteins at 20 °C, resulting in a significant decrease in thermal stability, which was reflected by a decrease in the transition temperature of more than 10 °C as well as a decrease in the calorimetric enthalpy of HSA-B compared to the HSA-N forms. The position of the DSC transition with the highest enthalpy likely corresponds to the thermal denaturation of domain II, due to its stabilization through interdomain interface interactions with domains I and III (**Fig. 1**). This statement is supported by the fact that the transition temperatures determined from Trp fluorescence measurements are higher than those obtained from ellipticity dependencies, strongly suggesting that conformation transition of the domain II begins after denaturation of domains I and III in the acidic pH region. These results are in agreement with findings obtained

by Muzammil and coworkers who showed that tertiary structure is more stable than secondary structure at low pH [74]. This conclusion is also in line with our observation that the fluorescence maximum of HSA-F is shifted to a lower wavelength in comparison with HSA-N indicating increased hydrophobicity, i.e. a single Trp in the domain II is apparently more buried in the protein structure [75]. (Albumin) HSA-F form represents a partially unfolded state with less secondary structure content in comparison with the normal physiological HSA-N form [76]. Structural disturbance of HSA-F form influences probably also the integrity of FAs binding sites which results in their weak stabilization effect at this pH region. The HSA-N form seems to be more compact and stable than the HSA-F form. Flora and coworkers showed that the largest structural changes at pH 7.2 occur above 60 °C which is consistent with our results [46]. However, they suggest that the denaturation of domain I takes place after the complete denaturation of domain II above 70 °C. In our case, both spectroscopic curves are almost identical which indicates the simultaneous denaturation of all domains which is consistent with the work of Ahmad [47]. In the case of HSA_{FA}-N, there is uneven stabilization of the domains which is reflected by the presence of a shoulder in the DSC curve. Considering that Trp fluorescence does not correspond to the position of this shoulder and that most FA binding sites (also with the highest affinity) are located in domain III, this transition thus likely represents the denaturation of domain III. Therefore, based on the obtained results, we conclude that the thermal denaturation of both HSA-N and HSA_{FA}-N forms proceeds in the following order: domain I ~ domain II < domain III. DSC scans of HSA-B and HSA_{FA}-B forms are characterized by the appearance of a new shoulder located on the higher temperature side of the main peak. The presence of the shoulder as well as differences between CD and Trp fluorescence results indicate structural rearrangement that occurs in the alkaline pH region. The N-B conformational transition has been shown to be accompanied by a decrease in α-helical content and inter-domain distances, which explains why the HSA-B form is less stable than the HSA-N form [27,32]. In addition, Qiu et al. showed that structural isomerization involves predominantly domains I and II while domain III is intact [27]. Along with the finding that the Trp fluorescence curve also correlates to the first observed DSC transition, it again suggests that denaturation of domain III occurs as the last one. Although the high enthalpies of the first thermal transition in the HSA-B and HSA_{FA}-B forms suggest that domain II unfolds as the first, our results do not allow to unequivocally determine the order of thermal denaturation of domains I and II in the HSA-B forms.

Biological implications. The concentration of albumins in human serum is within the range of 35-50 mg/ml [77]. The experimentally determined transition temperature above 65°C

for human serum albumin at 48 mg/ml implies sufficient thermal stability of albumins under physiological conditions [71]. The thermal denaturation model of HSA and HSA_{FA} presented in our work consists of a reversible step followed by one (HSA) or two (HSA_{FA}) consecutive step(s). In analogy with immunoglobulin G for which thermal denaturation is described by the same model as for HSA_{FA}, the first reversible step in protein thermal transition significantly increases the kinetic stability of the protein [52]. Additional stabilization of human serum albumin may play a role in the physiological environment of the bloodstream, where the protein is subjected to stringent forces and the presence of various ligands that may also have a destabilizing effect on albumin. A model that is able to correctly determine the thermodynamic and kinetic parameters can significantly help in the analysis of ligand binding to albumin from the point of view of localization of the binding sites in the protein structure as well as ligand affinity.

5. Conclusion

In conclusion, we show that the inconsistency of the results obtained in the studies of thermal denaturation of serum albumin in the literature is related to different sample quality between batches, methodological approaches and experimental conditions used in studies. The presence of FAs causes a more complex thermal denaturation of albumin. The thermal denaturation of albumin is strongly pH-dependent, even within a single conformational form. While the HSA unfolding pathway can be described by a two-step model, the temperature denaturation of HSA_{FA} appears to be a three-step process analogous to the thermal denaturation of IgG molecules [78,79]. Our findings also indicate that at neutral and basic pH, independent of the presence of FAs, domain III is the most stable domain of HSA. The identification of a proper model of thermal denaturation of HSA and HSA_{FA} allows correct determination of the thermodynamic and kinetic parameters connected with the human serum albumin thermal transitions in the presence of different ligands or in conjugation with therapeutic proteins. This can be particularly helpful in the development of HSA-based drug delivery systems.

Declaration of competing interest

The authors declare no competing interest.

Acknowledgements

This work was supported by Slovak Research and Development Agency through the project APVV-20-0340 and by the grant agency of the Ministry of Education, Science, Research, and

Sport of the Slovak Republic (grant no. VEGA 1/0074/22) and by the EU H2020-WIDESPREAD-05-2020 grant No. 952333, CasProt (Fostering high scientific quality in protein science in Eastern Slovakia). This publication is the result of the project implementation: Open scientific community for modern interdisciplinary research in medicine (Acronym: OPENMED), ITMS2014+: 313011V455 and BioPickmol, ITMS2014+: 313011AUW6 supported by the Operational Programme Integrated Infrastructure, funded by the ERDF.

References

[1] J.F. Foster, SOME ASPECTS OF THE STRUCTURE AND CONFORMATIONAL PROPERTIES OF SERUM ALBUMIN, in: V.M. Rosenoer, M. Oratz, M.A. Rothschild (Eds.), Albumin: Structure, Function and Uses, Pergamon, 1977: pp. 53–84. https://doi.org/10.1016/B978-0-08-019603-9.50010-7.

[2] G. Fanali, A. di Masi, V. Trezza, M. Marino, M. Fasano, P. Ascenzi, Human serum albumin: from bench to bedside, Mol Aspects Med. 33 (2012) 209–290. https://doi.org/10.1016/j.mam.2011.12.002.

[3] J. Ghuman, P.A. Zunszain, I. Petitpas, A.A. Bhattacharya, M. Otagiri, S. Curry, Structural basis of the drug-binding specificity of human serum albumin, J Mol Biol. 353 (2005) 38–52. https://doi.org/10.1016/j.jmb.2005.07.075.

[4] G. Kostandini, B.F. Mills, G.W. Norton, The Potential Impact of Tobacco Biopharming: The Case of Human Serum Albumin, American Journal of Agricultural Economics. 88 (2006) 671–679. https://doi.org/10.1111/j.1467-8276.2006.00887.x.

[5] J. Qi, Y. Zhang, Y. Gou, P. Lee, J. Wang, S. Chen, Z. Zhou, X. Wu, F. Yang, H. Liang, Multidrug Delivery Systems Based on Human Serum Albumin for Combination Therapy with Three Anticancer Agents, Mol. Pharmaceutics. 13 (2016) 3098–3105. https://doi.org/10.1021/acs.molpharmaceut.6b00277.

[6] D. Belej, Z. Jurasekova, M. Nemergut, G. Wagnieres, D. Jancura, V. Huntosova, Negligible interaction of [Ru(Phen)3]2+ with human serum albumin makes it promising for a reliable in vivo assessment of the tissue oxygenation, Journal of Inorganic Biochemistry. 174 (2017) 37–44. https://doi.org/10.1016/j.jinorgbio.2017.05.016.

[7] N. Abdollahpour, V. Soheili, M.R. Saberi, J. Chamani, Investigation of the Interaction Between Human Serum Albumin and Two Drugs as Binary and Ternary Systems, Eur J Drug Metab Pharmacokinet. 41 (2016) 705–721. https://doi.org/10.1007/s13318-015-0297-y.

[8] S. Khashkhashi-Moghadam, S. Ezazi-Toroghi, M. Kamkar-Vatanparast, P. Jouyaeian, P. Mokaberi, H. Yazdyani, Z. Amiri-Tehranizadeh, M. Reza Saberi, J. Chamani, Novel perspective into the interaction behavior study of the cyanidin with human serum albumin-holo transferrin complex: Spectroscopic, calorimetric and molecular modeling approaches, Journal of Molecular Liquids. 356 (2022) 119042. https://doi.org/10.1016/j.molliq.2022.119042.

[9] G. Sudlow, D.J. Birkett, D.N. Wade, The characterization of two specific drug binding sites on human serum albumin, Mol Pharmacol. 11 (1975) 824–832.

[10] A. Varshney, P. Sen, E. Ahmad, M. Rehan, N. Subbarao, R.H. Khan, Ligand binding strategies of human serum albumin: how can the cargo be utilized?, Chirality. 22 (2010) 77–87. https://doi.org/10.1002/chir.20709.

[11] N. Lomis, S. Westfall, L. Farahdel, M. Malhotra, D. Shum-Tim, S. Prakash, Human Serum Albumin Nanoparticles for Use in Cancer Drug Delivery: Process Optimization and In Vitro Characterization, Nanomaterials (Basel). 6 (2016) 116. https://doi.org/10.3390/nano6060116.

[12] S. D, C. J, E. Lr, Albumin as a versatile platform for drug half-life extension, Biochimica et Biophysica Acta. 1830 (2013). https://doi.org/10.1016/j.bbagen.2013.04.023.
[13] J. Feng, C. Zhao, L. Wang, L. Qu, H. Zhu, Z. Yang, G. An, H. Tian, C. Shou, Development of a novel albumin-based and maleimidopropionic acid-conjugated peptide with prolonged half-life and increased *in vivo* anti-tumor efficacy, Theranostics. 8 (2018) 2094–2106. https://doi.org/10.7150/thno.22069.
[14] M. Bern, K.M.K. Sand, J. Nilsen, I. Sandlie, J.T. Andersen, The role of albumin receptors in regulation of albumin homeostasis: Implications for drug delivery, J Control Release. 211 (2015) 144–162. https://doi.org/10.1016/j.jconrel.2015.06.006.
[15] G. Rabbani, E.J. Lee, K. Ahmad, M.H. Baig, I. Choi, Binding of Tolperisone Hydrochloride with Human Serum Albumin: Effects on the Conformation, Thermodynamics, and Activity of HSA, Mol Pharm. 15 (2018) 1445–1456. https://doi.org/10.1021/acs.molpharmaceut.7b00976.
[16] G. Rabbani, S.N. Ahn, Structure, enzymatic activities, glycation and therapeutic potential of human serum albumin: A natural cargo, Int J Biol Macromol. 123 (2019) 979–990. https://doi.org/10.1016/j.ijbiomac.2018.11.053.
[17] G. Rabbani, S.N. Ahn, Review: Roles of human serum albumin in prediction, diagnoses and treatment of COVID-19, Int J Biol Macromol. 193 (2021) 948–955. https://doi.org/10.1016/j.ijbiomac.2021.10.095.
[18] X.M. He, D.C. Carter, Atomic structure and chemistry of human serum albumin, Nature. 358 (1992) 209–215. https://doi.org/10.1038/358209a0.
[19] S. Sugio, A. Kashima, S. Mochizuki, M. Noda, K. Kobayashi, Crystal structure of human serum albumin at 2.5 Å resolution, Protein Engineering, Design and Selection. 12 (1999) 439–446. https://doi.org/10.1093/protein/12.6.439.
[20] A.A. Bhattacharya, T. Grüne, S. Curry, Crystallographic analysis reveals common modes of binding of medium and long-chain fatty acids to human serum albumin, J Mol Biol. 303 (2000) 721–732. https://doi.org/10.1006/jmbi.2000.4158.
[21] I. Petitpas, T. Grüne, A.A. Bhattacharya, S. Curry, Crystal structures of human serum albumin complexed with monounsaturated and polyunsaturated fatty acids, J Mol Biol. 314 (2001) 955–960. https://doi.org/10.1006/jmbi.2000.5208.
[22] P. Ascenzi, M. Fasano, Allostery in a monomeric protein: the case of human serum albumin, Biophys Chem. 148 (2010) 16–22. https://doi.org/10.1016/j.bpc.2010.03.001.
[23] S. Curry, H. Mandelkow, P. Brick, N. Franks, Crystal structure of human serum albumin complexed with fatty acid reveals an asymmetric distribution of binding sites, Nat Struct Biol. 5 (1998) 827–835. https://doi.org/10.1038/1869.
[24] S. Curry, P. Brick, N.P. Franks, Fatty acid binding to human serum albumin: new insights from crystallographic studies, Biochim Biophys Acta. 1441 (1999) 131–140. https://doi.org/10.1016/s1388-1981(99)00148-1.
[25] C. Leggio, L. Galantini, N.V. Pavel, About the albumin structure in solution: cigar Expanded form versus heart Normal shape, Phys. Chem. Chem. Phys. 10 (2008) 6741–6750. https://doi.org/10.1039/B808938H.
[26] M. Dockal, D.C. Carter, F. Rüker, Conformational transitions of the three recombinant domains of human serum albumin depending on pH, J Biol Chem. 275 (2000) 3042–3050. https://doi.org/10.1074/jbc.275.5.3042.
[27] W. Qiu, L. Zhang, O. Okobiah, Y. Yang, L. Wang, D. Zhong, A.H. Zewail, Ultrafast Solvation Dynamics of Human Serum Albumin: Correlations with Conformational Transitions and Site-Selected Recognition, J. Phys. Chem. B. 110 (2006) 10540–10549. https://doi.org/10.1021/jp055989w.
[28] K. Baler, O.A. Martin, M.A. Carignano, G.A. Ameer, J.A. Vila, I. Szleifer, Electrostatic Unfolding and Interactions of Albumin Driven by pH Changes: A Molecular Dynamics Study, J. Phys. Chem. B. 118 (2014) 921–930. https://doi.org/10.1021/jp409936v.
[29] M. Ishtikhar, G. Rabbani, R.H. Khan, Interaction of 5-fluoro-5′-deoxyuridine with human serum albumin under physiological and non-physiological condition: A biophysical investigation,

Colloids and Surfaces B: Biointerfaces. 123 (2014) 469–477. https://doi.org/10.1016/j.colsurfb.2014.09.044.
[30] M. Ishtikhar, G. Rabbani, S. Khan, R.H. Khan, Biophysical investigation of thymoquinone binding to 'N' and 'B' isoforms of human serum albumin: exploring the interaction mechanism and radical scavenging activity, RSC Adv. 5 (2015) 18218–18232. https://doi.org/10.1039/C4RA09892G.
[31] N. Díaz, D. Suárez, Role of the Protonation State on the Structure and Dynamics of Albumin, J. Chem. Theory Comput. 12 (2016) 1972–1988. https://doi.org/10.1021/acs.jctc.5b01001.
[32] B. Honoré, A.O. Pedersen, Conformational changes in human serum albumin studied by fluorescence and absorption spectroscopy. Distance measurements as a function of pH and fatty acids, Biochem J. 258 (1989) 199–204. https://doi.org/10.1042/bj2580199.
[33] E.J. Cohn, L.E. Strong, W.L. Hughes, D.J. Mulford, J.N. Ashworth, M. Melin, H.L. Taylor, Preparation and Properties of Serum and Plasma Proteins. IV. A System for the Separation into Fractions of the Protein and Lipoprotein Components of Biological Tissues and Fluids1a,b,c,d, J. Am. Chem. Soc. 68 (1946) 459–475. https://doi.org/10.1021/ja01207a034.
[34] J.T. Edsall, Stabilization of serum albumin to heat, and inactivation of the hepatitis virus, Vox Sang. 46 (1984) 338–340. https://doi.org/10.1111/j.1423-0410.1984.tb00096.x.
[35] K. Tanaka, E.M. Shigueoka, E. Sawatani, G.A. Dias, F. Arashiro, T.C. Campos, H.C. Nakao, Purification of human albumin by the combination of the method of Cohn with liquid chromatography, Braz J Med Biol Res. 31 (1998) 1383–1388. https://doi.org/10.1590/s0100-879x1998001100003.
[36] R. Raoufinia, A. Mota, N. Keyhanvar, F. Safari, S. Shamekhi, J. Abdolalizadeh, Overview of Albumin and Its Purification Methods, Adv Pharm Bull. 6 (2016) 495–507. https://doi.org/10.15171/apb.2016.063.
[37] R.J. Gerety, D.L. Aronson, Plasma derivatives and viral hepatitis, Transfusion. 22 (1982) 347–351. https://doi.org/10.1046/j.1537-2995.1982.22583017454.x.
[38] C.L. Darcel, M.S. Kaldy, Further evidence for the heterogeneity of serum albumin, Comp Biochem Physiol B. 85 (1986) 15–22. https://doi.org/10.1016/0305-0491(86)90215-4.
[39] G. Barone, S. Capasso, P.D. Vecchio, C.D. Sena, D. Fessas, C. Giancola, G. Graziano, P. Tramonti, Thermal denaturation of bovine serum albumin and its oligomers and derivativespH dependence, Journal of Thermal Analysis. 45 (1995) 1255.
[40] N. Qu, Y. Sun, Y. Li, F. Hao, P. Qiu, L. Teng, J. Xie, Y. Gao, Docetaxel-loaded human serum albumin (HSA) nanoparticles: synthesis, characterization, and evaluation, BioMedical Engineering OnLine. 18 (2019) 11. https://doi.org/10.1186/s12938-019-0624-7.
[41] S. Muzammil, Y. Kumar, S. Tayyab, Anion-induced stabilization of human serum albumin prevents the formation of intermediate during urea denaturation, Proteins. 40 (2000) 29–38. https://doi.org/10.1002/(sici)1097-0134(20000701)40:1<29::aid-prot50>3.0.co;2-p.
[42] B. Ahmad, M.Z. Ahmed, S.K. Haq, R.H. Khan, Guanidine hydrochloride denaturation of human serum albumin originates by local unfolding of some stable loops in domain III, Biochim Biophys Acta. 1750 (2005) 93–102. https://doi.org/10.1016/j.bbapap.2005.04.001.
[43] R. Wetzel, M. Becker, J. Behlke, H. Billwitz, S. Böhm, B. Ebert, H. Hamann, J. Krumbiegel, G. Lassmann, Temperature behaviour of human serum albumin, Eur J Biochem. 104 (1980) 469–478. https://doi.org/10.1111/j.1432-1033.1980.tb04449.x.
[44] G.A. Picó, Thermodynamic features of the thermal unfolding of human serum albumin, Int J Biol Macromol. 20 (1997) 63–73. https://doi.org/10.1016/s0141-8130(96)01153-1.
[45] J.M. Sanchez-Ruiz, Theoretical analysis of Lumry-Eyring models in differential scanning calorimetry, Biophys J. 61 (1992) 921–935.
[46] K. Flora, J.D. Brennan, G.A. Baker, M.A. Doody, F.V. Bright, Unfolding of acrylodan-labeled human serum albumin probed by steady-state and time-resolved fluorescence methods., Biophys J. 75 (1998) 1084–1096.
[47] B. Ahmad, G. Muteeb, P. Alam, A. Varshney, N. Zaidi, M. Ishtikhar, G. Badr, M.H. Mahmoud, R.H. Khan, Thermal induced unfolding of human serum albumin isomers: Assigning residual α

helices to domain II, International Journal of Biological Macromolecules. 75 (2015) 447–452. https://doi.org/10.1016/j.ijbiomac.2015.02.003.
[48] M. Rezaei-Tavirani, S.H. Moghaddamnia, B. Ranjbar, M. Amani, S.-A. Marashi, Conformational Study of Human Serum Albumin in Pre-denaturation Temperatures by Differential Scanning Calorimetry, Circular Dichroism and UV Spectroscopy, BMB Reports. 39 (2006) 530–536. https://doi.org/10.5483/BMBRep.2006.39.5.530.
[49] V. Mohan, B. Sengupta, A. Acharyya, R. Yadav, N. Das, P. Sen, Region-Specific Double Denaturation of Human Serum Albumin: Combined Effects of Temperature and GnHCl on Structural and Dynamical Responses, ACS Omega. 3 (2018) 10406–10417. https://doi.org/10.1021/acsomega.8b00967.
[50] T. Kosa, T. Maruyama, M. Otagiri, Species differences of serum albumins: II. Chemical and thermal stability, Pharm Res. 15 (1998) 449–454. https://doi.org/10.1023/a:1011932516717.
[51] B. Sengupta, N. Das, P. Sen, Elucidation of μs dynamics of domain-III of human serum albumin during the chemical and thermal unfolding: A fluorescence correlation spectroscopic investigation, Biophys Chem. 221 (2017) 17–25. https://doi.org/10.1016/j.bpc.2016.11.006.
[52] E. Sedlák, J.V. Schaefer, J. Marek, P. Gimeson, A. Plückthun, Advanced analyses of kinetic stabilities of iggs modified by mutations and glycosylation, Protein Sci. 24 (2015) 1100–1113. https://doi.org/10.1002/pro.2691.
[53] E. Sedlák, R. Varhač, A. Musatov, N.C. Robinson, The Kinetic Stability of Cytochrome c Oxidase: Effect of Bound Phospholipid and Dimerization, Biophys J. 107 (2014) 2941–2949. https://doi.org/10.1016/j.bpj.2014.10.055.
[54] J. Lahiri, S. Sandhu, B.G. Levine, M. Dantus, Human Serum Albumin Dimerization Enhances the S2 Emission of Bound Cyanine IR806, J Phys Chem Lett. 13 (2022) 1825–1832. https://doi.org/10.1021/acs.jpclett.1c03735.
[55] U. Anand, S. Mukherjee, Binding, unfolding and refolding dynamics of serum albumins, Biochimica et Biophysica Acta (BBA) - General Subjects. 1830 (2013) 5394–5404. https://doi.org/10.1016/j.bbagen.2013.05.017.
[56] A. Bhattacharya, R. Prajapati, S. Chatterjee, T.K. Mukherjee, Concentration-dependent reversible self-oligomerization of serum albumins through intermolecular β-sheet formation, Langmuir. 30 (2014) 14894–14904. https://doi.org/10.1021/la5034959.
[57] A. Chubarov, A. Spitsyna, O. Krumkacheva, D. Mitin, D. Suvorov, V. Tormyshev, M. Fedin, M.K. Bowman, E. Bagryanskaya, Reversible Dimerization of Human Serum Albumin, Molecules. 26 (2021) 108. https://doi.org/10.3390/molecules26010108.
[58] N.A. Bushmarina, I.M. Kuznetsova, A.G. Biktashev, K.K. Turoverov, V.N. Uversky, Partially folded conformations in the folding pathway of bovine carbonic anhydrase II: a fluorescence spectroscopic analysis, Chembiochem. 2 (2001) 813–821. https://doi.org/10.1002/1439-7633(20011105)2:11<813::AID-CBIC813>3.0.CO;2-W.
[59] I.M. Kuznetsova, O.V. Stepanenko, K.K. Turoverov, L. Zhu, J.M. Zhou, A.L. Fink, V.N. Uversky, Unraveling multistate unfolding of rabbit muscle creatine kinase, Biochim Biophys Acta. 1596 (2002) 138–155. https://doi.org/10.1016/s0167-4838(02)00212-1.
[60] I.M. Kuznetsova, K.K. Turoverov, V.N. Uversky, Use of the phase diagram method to analyze the protein unfolding-refolding reactions: fishing out the “invisible” intermediates, J Proteome Res. 3 (2004) 485–494. https://doi.org/10.1021/pr034094y.
[61] G. Rabbani, M.H. Baig, E.J. Lee, W.-K. Cho, J.Y. Ma, I. Choi, Biophysical Study on the Interaction between Eperisone Hydrochloride and Human Serum Albumin Using Spectroscopic, Calorimetric, and Molecular Docking Analyses, Mol Pharm. 14 (2017) 1656–1665. https://doi.org/10.1021/acs.molpharmaceut.6b01124.
[62] G. Rabbani, M.H. Baig, A.T. Jan, E. Ju Lee, M.V. Khan, M. Zaman, A.-E. Farouk, R.H. Khan, I. Choi, Binding of erucic acid with human serum albumin using a spectroscopic and molecular docking study, Int J Biol Macromol. 105 (2017) 1572–1580. https://doi.org/10.1016/j.ijbiomac.2017.04.051.

[63] B. Farruggia, F. Rodriguez, R. Rigatuso, G. Fidelio, G. Picó, The Participation of Human Serum Albumin Domains in Chemical and Thermal Unfolding, J Protein Chem. 20 (2001) 81–89. https://doi.org/10.1023/A:1011000317042.
[64] A. Michnik, K. Michalik, A. Kluczewska, Z. Drzazga, Comprative DSC study of human and bovin serum albumin, Journal of Thermal Analysis and Calorimetry - J THERM ANAL CALORIM. 84 (2006) 113–117. https://doi.org/10.1007/s10973-005-7170-1.
[65] M.S. Celej, S.A. Dassie, M. González, M.L. Bianconi, G.D. Fidelio, Differential scanning calorimetry as a tool to estimate binding parameters in multiligand binding proteins, Anal Biochem. 350 (2006) 277–284. https://doi.org/10.1016/j.ab.2005.12.029.
[66] E. Sedlák, L. Ziegler, D.J. Kosman, P. Wittung-Stafshede, In vitro unfolding of yeast multicopper oxidase Fet3p variants reveals unique role of each metal site, Proc Natl Acad Sci U S A. 105 (2008) 19258–19263. https://doi.org/10.1073/pnas.0806431105.
[67] K. Aoki, S. Sakurai, M. Murata, T. Ito, H. Terada, K. Hiramatsu, Studies on components 1' (modified monomer) and 2 (dimer) formed during heat-treatment of bovine serum albumin, Colloid & Polymer Sci. 262 (1984) 470–476. https://doi.org/10.1007/BF01412043.
[68] P.D. Ross, A. Shrake, Decrease in stability of human albumin with increase in protein concentration., Journal of Biological Chemistry. 263 (1988) 11196–11202. https://doi.org/10.1016/S0021-9258(18)37941-9.
[69] J. Brandt, L.-O. Andersson, Heat Denaturation of Human Serum Albumin. Migration of Bound Fatty Acids, International Journal of Peptide and Protein Research. 8 (1976) 33–37. https://doi.org/10.1111/j.1399-3011.1976.tb02478.x.
[70] S. Gumpen, P.O. Hegg, H. Martens, Thermal stability of fatty acid-serum albumin complexes studied by differential scanning calorimetry, Biochim Biophys Acta. 574 (1979) 189–196. https://doi.org/10.1016/0005-2760(79)90001-8.
[71] A. Shrake, J.S. Finlayson, P.D. Ross, Thermal stability of human albumin measured by differential scanning calorimetry. I. Effects of caprylate and N-acetyltryptophanate, Vox Sang. 47 (1984) 7–18. https://doi.org/10.1111/j.1423-0410.1984.tb01556.x.
[72] M.W. Yu, J.S. Finlayson, Stabilization of human albumin by caprylate and acetyltryptophanate, Vox Sang. 47 (1984) 28–40. https://doi.org/10.1111/j.1423-0410.1984.tb01558.x.
[73] A. Shrake, P.D. Ross, Biphasic denaturation of human albumin due to ligand redistribution during unfolding., Journal of Biological Chemistry. 263 (1988) 15392–15399. https://doi.org/10.1016/S0021-9258(19)37601-X.
[74] S. Muzammil, Y. Kumar, S. Tayyab, Molten globule-like state of human serum albumin at low pH, Eur J Biochem. 266 (1999) 26–32. https://doi.org/10.1046/j.1432-1327.1999.00810.x.
[75] E.A. Burstein, N.S. Vedenkina, M.N. Ivkova, Fluorescence and the location of tryptophan residues in protein molecules, Photochem Photobiol. 18 (1973) 263–279. https://doi.org/10.1111/j.1751-1097.1973.tb06422.x.
[76] A.K. Shaw, S.K. Pal, Resonance energy transfer and ligand binding studies on pH-induced folded states of human serum albumin, Journal of Photochemistry and Photobiology B: Biology. 90 (2008) 187–197. https://doi.org/10.1016/j.jphotobiol.2008.01.001.
[77] T. Peters, All About Albumin: Biochemistry, Genetics and Medical Applications., CA: Academic Press Limited., San Diego, 1996.
[78] M. Nemergut, G. Zoldak, J.V. Schaefer, F. Kast, P. Miskovsky, A. Pluckthun, E. Sedlak, Analysis of IgG kinetic stability by differential scanning calorimetry, probe fluorescence and light scattering, Protein Sci. 26 (2017) 2229–2239. https://doi.org/10.1002/pro.3278.
[79] J.V. Schaefer, E. Sedlak, F. Kast, M. Nemergut, A. Pluckthun, Modification of the kinetic stability of immunoglobulin G by solvent additives, MAbs. 10 (2018) 607–623. https://doi.org/10.1080/19420862.2018.1450126.